Chemical Science

ROYAL SOCIETY OF CHEMISTRY

EDGE ARTICLE

View Article Online
View Journal | View Issue

Cite this: *Chem. Sci.*, 2024, **15**, 18093

All publication charges for this article have been paid for by the Royal Society of Chemistry

Received 8th August 2024
Accepted 7th October 2024

DOI: 10.1039/d4sc05337k

rsc.li/chemical-science

Is aromaticity loss necessary for transition-metal promoted arene–alkene cycloadditions?†

João V. Schober, * Croix J. Laconsay and Judy I. Wu *

Computed gas-phase reaction profiles for Diels–Alder reactions, nucleus-independent chemical shifts, and bonding analyses for substituted and metal complexed, η^2-, η^4-, η^6-coordinated arenes reveal that dearomatization is necessary for arenes to exhibit ene- and diene-like reactivity. Substituted arenes and η^6-arenes exhibit high free energy barriers towards cycloaddition reactions, but strongly dearomatized η^2- and η^4-arenes can display low free energy barriers (~20 kcal mol^{-1} or less) for [4 + 2] cycloaddition reactions.

Introduction

Arenes are rarely envisioned as dienes or dienophiles for Diels–Alder reactions because of the energetic penalty for disrupting aromaticity. For this reason, known examples of arene Diels–Alder reactions typically involve harsh conditions (*i.e.*, high temperature and pressure),[1,2] photoreactions,[3–6] strained scaffolds,[7,8] or the use of highly potent dienes or dienophiles.[9] Transition metal coordination can profoundly alter the reactivity of aromatic systems,[10–14] and in some cases, instill diene- or ene-like reactivity in much milder conditions.[15–19] It was suggested that increased diene- and ene-like reactivity is linked to a loss of aromaticity in the metal coordinated arene, but such relationships have only been speculated. In this computational investigation, we show that diene- and ene-like reactivity in transition metal coordinated arenes can only be expected when the metal complexed arene displays a notable degree of aromaticity loss.

Even though examples of dihapto (η^2) and tetrahapto (η^4) coordinated arenes showing diene- and ene-like reactivity are known, the role of aromaticity loss of the coordinated arene in driving such reactivity has never been quantified. In a series of papers, Harman *et al.* reported that η^2-arenes, heteroarenes, and fused arenes could mimic the cycloaddition reactivity of dienes and undergo Diels–Alder reactions (Fig. 1a and b)[11,16–18,20] Cooper *et al.* found that η^4-Mn(CO)$_3$-benzene could undergo two sequential electrophilic addition steps followed by ring closure to yield cyclohexadienyl complexes *via* a [2 + 2 + 2] cycloaddition (Fig. 1c).[15] Fe(CO)$_3$ complexes of tropone show enone-like reactivity.[21,22] Yet, not all metal-complexed arenes show diene- or ene-like reactivity. η^6-Cr(CO)$_3$, η^6-Mn(CO)$_3^+$, η^6-FeCp$^+$, and η^6-RuCp$^+$ readily undergo nucleophilic substitution and addition reactions to form substituted benzenes and cyclohexadienes, but do not show diene- or ene-like reactivity.[10] Likewise, substituents can effectively promote electrophilic and nucleophilic reactions in arenes,[23] but do not show diene- or ene-like reactivity either. What are the necessary criteria for making arenes react like dienes and dienophiles?

Results and discussion

We selected three aromatic systems (benzene, naphthalene, indole) and first examined the dearomatization effects of η^2 (**1–8**), η^4 (**9–14**), and η^6 (**15–17**) coordination, as quantified by dissected nucleus-independent chemical shifts,[24] NICS(1)$_{zz}$, a magnetic index of aromaticity that measures the diatropicity and paratropicity of a system (Fig. 2). Negative NICS(1)$_{zz}$ values indicate aromaticity (diatropicity), and positive NICS(1)$_{zz}$ values

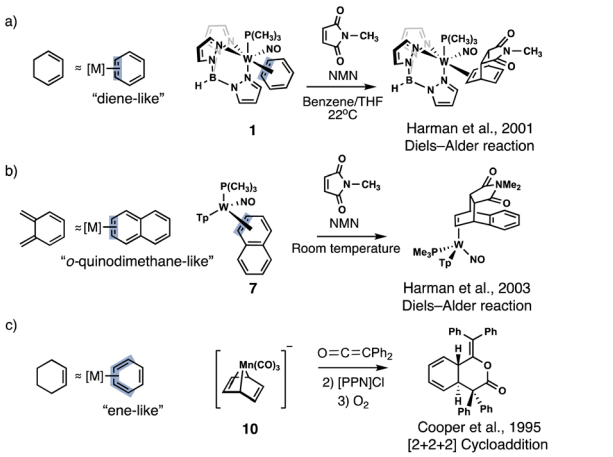

Fig. 1 Examples of η^2- and η^4- arenes and fused arenes showing diene- and ene-like reactivity.

Department of Chemistry, University of Houston, Houston, TX 77204, USA. E-mail: jiwu@central.uh.edu; jvoliveisoares@uh.edu

† Electronic supplementary information (ESI) available. See DOI: https://doi.org/10.1039/d4sc05337k

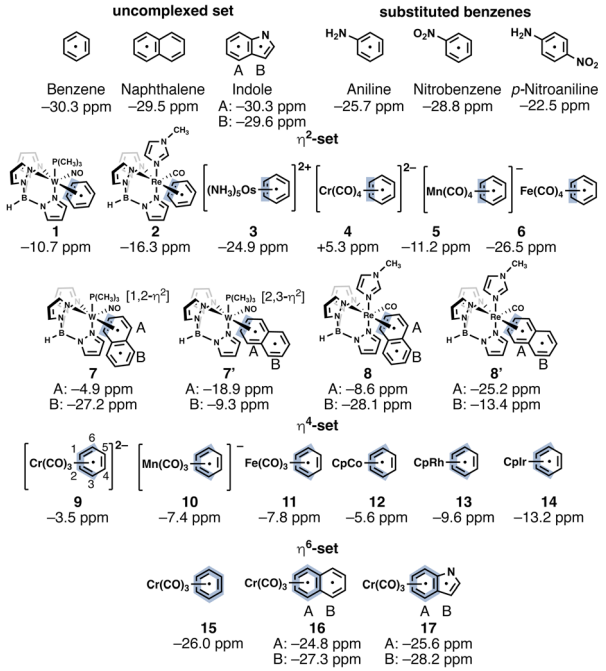

Fig. 2 NICS(1)$_{zz}$ values for selected arenes and their η^2-, η^4-, and η^6-complexes.

indicate antiaromaticity (paratropicity). Noting that a nearby transition-metal could cause deshielding effects on the computed NICS values,[25] NICS probes were placed 1 Å above the π-ring opposite to the transition-metal coordinating side. The complexes shown in Fig. 2 are organized based on increasing effective nuclear charge of the metal (left to right across a Row and up to down across a Group). Large negative NICS(1)$_{zz}$ values indicate that all of the uncomplexed parent compounds are strongly aromatic (Fig. 2). Computed NICS(1)$_{zz}$ values for selected substituted benzenes: aniline (−25.7 ppm), nitrobenzene (−28.8 ppm), and *p*-nitrobenzene (−22.5 ppm) are only modestly less negative compared to benzene and exemplify the robustness of aromaticity towards ring substitution.[26] A small decrease in diatropicity occurs only when push–pull groups are placed strategically around the arene; and even then, there is only modest aromaticity loss.

The η^2-benzenes (**1–6**) exhibit a range of NICS(1)$_{zz}$ values. Going across a row, the series: **1** (−10.7 ppm), **2** (−16.3 ppm), **3** (−24.9 ppm) (W → Re → Os), and the series: **4** (+5.3 ppm), **5** (−11.2 ppm), **6** (−26.5 ppm) (Cr → Mn → Fe), both show increasing diatropicity at the arene as the metal identity shifts from an early to late transition metal. Sums of Wiberg Bond Index (WBI)[27] values for the two metal-carbon contacts in each of the complexes decrease in the order: **1** (sum of WBI = 1.23, W) > **2** (1.17, Re) > **3** (0.82, Os) (Row 6), and **4** (1.03, Cr) > **5** (0.92, Mn) > **6** (0.54, Fe) (Row 4), suggesting that metals with a lower effective nuclear charge have stronger back-bonding interactions with the arene (*i.e.*, metal dπ orbital to arene pπ*). These findings are consistent with prior studies showing that **1** and **2** readily undergo Diels–Alder reactions with *N*-methylmaleimide (NMM) at room temperature, while **3** is unreactive.[16,17]

Fused arenes also can be activated for electrophilic addition by η^2-coordination. Harman *et al.* reported a Diels–Alder reactions for **7** with NMM.[18] The authors speculated that the thermodynamically favored 1,2-η^2-coordinated species, **7**, first ring walks to a 2,3-η^2-binding mode over a ∼19 kcal mol^{-1} barrier, and then NMM adds to the complexed ring (ring A, see **7′** in Fig. 2 and S2†).[18] Experiments carried out at elevated temperatures produced the cycloadduct with shorter reaction times.[18] Computed NICS(1)$_{zz}$ values for the 2,3-η^2-binding mode of **7** (ring A: −4.9 ppm, ring B: −27.2 ppm) and **7′** (ring A: −18.9 ppm, ring B: −9.3 ppm) suggest that ring walking from a 1,2-η^2 to a 2,3-η^2 binding mode is a relevant step. In **7**, adding NMM to ring A disrupts aromaticity in ring B (ring B in adduct: −1.3 ppm). But in **7′**, adding NMM to ring A restores aromaticity in ring B (ring B in adduct: −30.9 ppm). No Diels–Alder reactions were observed for **8** with NMM.[18,28] Computed NICS(1)$_{zz}$ values for **8′** (ring A: −25.2 ppm, ring B: −13.4 ppm) reveal a strongly aromatic ring A, which may explain the absence of a Diels–Alder reaction.

The η^4-benzenes (**9–14**) all show largely reduced diatropicities as the coordinated ring distorts from planarity. To estimate the NICS(1)$_{zz}$ values, an "out-of-plane" tensor component (*zz*) was defined by placing carbons C1, C2, C4, and C5 in the *xy* plane (see ring carbon numbering for **9**, Fig. 2). Going across Row 4: **9** (−3.5 ppm), **10** (−7.4 ppm), **11** (−7.8 ppm) (Cr → Mn → Fe), and down Group 9: **12** (−5.6 ppm), **13** (−9.6 ppm), **14** (−13.2 ppm) (Co → Rh → Ir), increased effective nuclear charge is accompanied by a more negative NICS(1)$_{zz}$ values. Since all of the η^4-arenes are nonplanar, we realize that the trends of the estimated NICS(1)$_{zz}$ values do not necessarily reflect changes in aromaticity. Nevertheless, it is reasonable to expect that all of the η^4-arenes are largely dearomatized.

The η^6-arenes (**15-17**) show minimal dearomatization (Fig. 2). Complexation to the electron-withdrawing Cr(CO)$_3$ group has been shown to activate arenes towards nucleophilic addition.[29] Yet, known reactions typically involve the formation of an η^5-coordinated complex and the η^6-binding mode is not the reacting species. Though, notably, it has been pointed out that Pauli repulsion lowering contributes to the interaction energies in different Ru moieties η^6-coordinated to coronulene.[30] In agreement with prior studies,[31] **15** (NICS(1)$_{zz}$ = −26.0 ppm) is nearly as aromatic as benzene (−30.3 ppm). The computed NICS(1)$_{zz}$ values for **16** (ring A: −24.8 ppm, ring B: −27.3 ppm) are comparable to those of naphthalene (−29.5 ppm), and those for **17** (ring A: −25.6 ppm, ring B: −28.2 ppm) are comparable to indole (ring A: −30.3 ppm, ring B: −29.6 ppm). All three η^6-complexes show only a slight decrease in negative NICS(1)$_{zz}$ values for the complexed arene (ring A); in **16** and **17**, ring B retains aromaticity and thus is unlikely to show "diene-like" reactivity. Hydrogenation and substitution reactions for **16** and **17** have been observed,[32,33] but their dearomatized analogs are even more reactive. This is consistent with experiments showing that tricarbonyl(naphthoquinone)chromium complexes could add to cyclic and acyclic dienes giving *endo* Diels–Alder products in good yield.[33]

We further note that the computed NICS(1)$_{zz}$ values for complexes **1-8**, **7′**, **8′**, **15**, **16**, benzene, naphthalene, and the

substituted benzenes (aniline, nitrobenzene, and *p*-nitroaniline) correlate satisfactorily with geometric indices of aromaticity, based on computed harmonic oscillator measure of aromaticity (HOMA)[34] values ($r^2 = 0.771$) (see data in the ESI†).

We next computed gas-phase reaction profiles for Diels–Alder reactions for benzene, *p*-nitroaniline, and selected η^2-, η^4- and η^6-arenes. Activation free energy barriers ($\Delta G^{\ddagger}$) were calculated based on the energy of the transition state structure relative to the σ-complex of the reactants. Since some of the reactions studied can proceed in an *endo* or *exo* fashion, we show the lower energy reaction pathway in Fig. 3a–d and include data for the alternative pathway in the ESI.† The reaction profile for a Diels–Alder reaction for benzene and cyclopentadiene is endothermic and reveals a high barrier ($\Delta G^{\ddagger}$ = 46.9 kcal mol^{-1}, Fig. 3a). This is comparable to the computed Diels–Alder reaction barrier for *p*-nitroaniline and cyclopentadiene, which also shows a high barrier ($\Delta G^{\ddagger}$ = 41.0 kcal mol^{-1}, *endo*, Fig. 3a), as anticipated by the largely intact aromatic character of the substituted arene. Computed HOMO and LUMO energies for benzene and *p*-nitroaniline reveal a lower HOMO–LUMO energy gap for *p*-nitroaniline, consistent with its higher reactivity (Table 1).

Computed energy profiles of Diels–Alder reactions for NMM with benzene and the η^2-benzenes (**1**–**3**) show decreasing $\Delta G^{\ddagger}$ values for benzene (38.3 kcal mol^{-1}) > **3** (32.8 kcal mol^{-1}, *endo*) > **2** (23.3 kcal mol^{-1}, *exo*) > **1** (22.9 kcal mol^{-1}, *exo*) (Fig. 3b), which is consistent with decreasing aromatic character of the arene ring: benzene > **3** > **2** > **1** (*cf.* Fig. 2b). Dearomatization prompts an earlier transition state, as suggested by the longer incipient C–C bonds of the transition state structures of **1** > **2** > **3** (Fig. 4). These findings are consistent with the observed "diene" reactivity of **1** and **2** *versus* the unreactive **3**.[16,17] Notably, the computed HOMO–LUMO energy gaps for **1** (3.46 eV), **2** (4.10 eV), and **3** (3.37 eV) are all lower than that of benzene (5.46 eV) (Table 1). Yet, there is no clear relationship between the HOMO–LUMO energy gaps of **1**–**3** and their computed Diels–Alder reaction barriers; **3** exhibits a lower HOMO–LUMO energy gap than **1** and **2** (Table 1), but a higher reaction barrier (Fig. 3b). In this regard, computed NICS(1)$_{zz}$ values, which quantify the extent of aromaticity loss, appear to be a more effective predictor for "diene-like" reactivity for η^2-coordinated species—less aromatic species are more reactive and exhibit lower Diels–Alder reaction barriers.

We examined Harman *et al.*'s proposal that a 2,3-η^2-coordinated naphthalene could mimic the cycloaddition reactivity of an *o*-quinodimethane. Cycloaddition adducts were reported for a hypothesized intermediate **7′** reacting with NMM. Indeed, the computed Diels–Alder reaction barrier for **7′** with NMM at the metal complexed ring (ring A) ($\Delta G^{\ddagger}$ = 10.6 kcal mol^{-1}, *exo*, Fig. 3c) is reasonably low. For comparison, the computed barrier for cycloaddition to the uncomplexed ring (ring B) (29.7 kcal mol^{-1}, *exo*) is much higher. These results are consistent with experimental observations of cycloaddition occurring at the complexed ring (ring A). In sharp contrast, computed Diels–Alder reaction barriers for an η^6-naphthalene complex, **16**, and NMM ($\Delta G^{\ddagger}$ = 31.0 kcal mol^{-1}, *endo*, Fig. 3c) is comparable to that of naphthalene with NMM ($\Delta G^{\ddagger}$ =

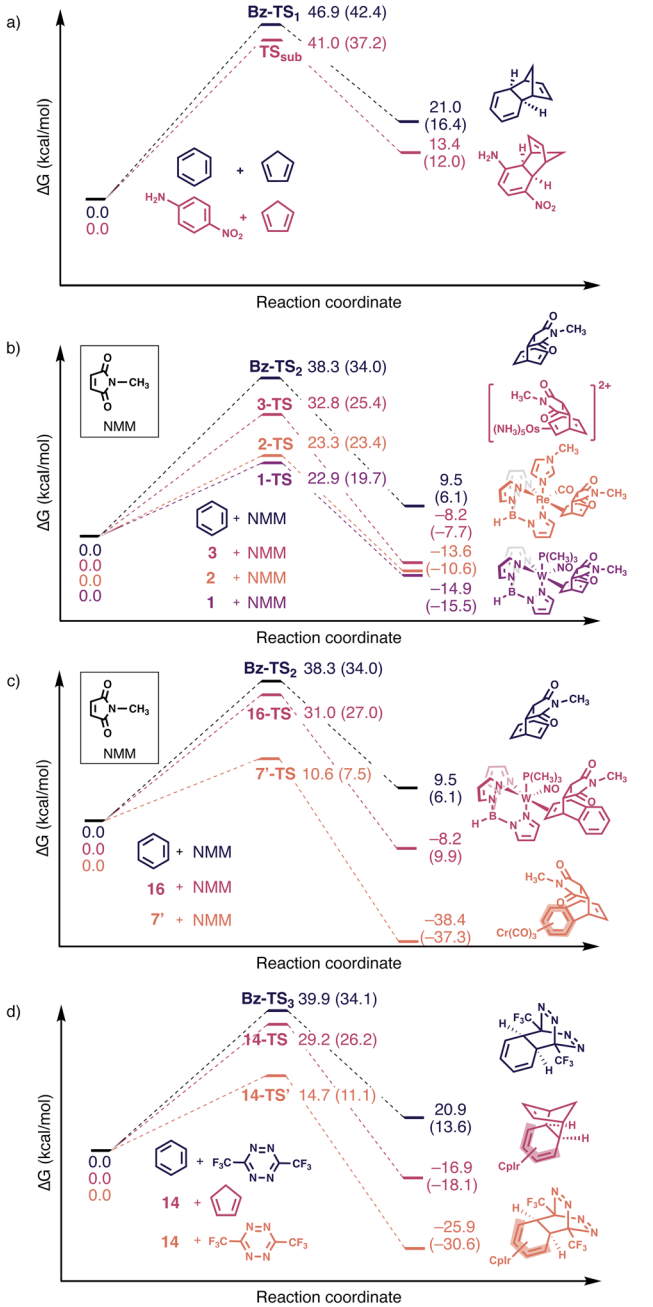

Fig. 3 Computed reaction profiles for Diels–Alder reactions at ωB97X-D/def2-TZVPP//ωB97X-D/def2-SVP. Single-point energies at DLPNO-CCSD(T)/def2-TZVPP//ωB97X-D/def2-SVP are in parenthesis. *Cf.* Fig. 4 shows computed transition state structures. All reaction barriers are computed relative to a σ-complex of the reactants.

32.5 kcal mol^{-1}, *endo*). This suggests that the uncomplexed "diene" fragment of **16** does not display diene reactivity (note that ring B remains largely aromatic, see Fig. 2, η^6-set). Both **7′** (2.43 eV) and **16** (2.85 eV), exhibit narrower HOMO–LUMO energy gaps than naphthalene (4.61 eV) (Table 1), which further exemplifies that aromaticity loss is obligatory for complexed arenes to show "diene-like" reactivity. Even though Cr(CO)$_3$ coordination activates **16** for nucleophilic addition,[29] this has

Table 1 Computed HOMO and LUMO energies and HOMO–LUMO energy gaps (ΔE_{H-L}) (in eV) of selected compounds

Compound	HOMO	LUMO	ΔE_{H-L}
Benzene	−8.49	−3.00	5.49
p-Nitroaniline	−7.84	−3.37	4.47
1	−5.54	−2.08	3.46
2	−5.47	−1.37	4.10
3	−13.80	−10.4	3.37
14	−6.40	−2.96	3.44
Naphthalene	−7.43	−2.82	4.61
7′	−5.07	−2.64	2.43
16	−7.04	−4.19	2.85

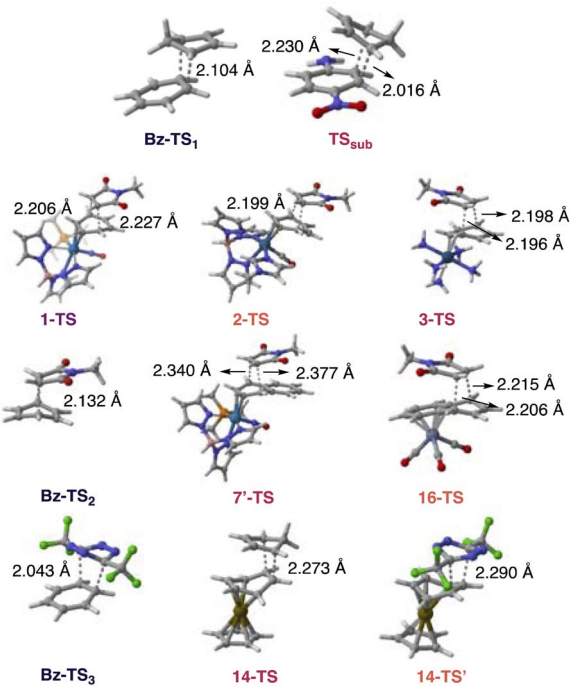

Fig. 4 Computed transition state structures for the Diels–Alder reactions shown in Fig. 3 at ωB97X-D/def2-SVP. Transition structures including only one bond length denotes that both forming bond lengths are identical.

little effect on promoting "diene-like" reactivity as the uncomplexed ring remains largely aromatic.

The η^4-benzenes have a preference for inverse electron-demand Diels–Alder reactions (Fig. 3d) as the uncomplexed "ene" fragment is strained (*i.e.*, like that of 7-norbornadiene) and electron-rich.[19] Computed energy profiles of Diels–Alder reactions for **14** with cyclopentadiene ($\Delta G^{\ddagger}$ = 29.2 kcal mol^{-1}, *endo*) *versus* with bis(trifluoromethyl)tetrazine ($\Delta G^{\ddagger}$ = 14.7 kcal mol^{-1}, inverse electron-demand) reveal a lower barrier for the latter (Fig. 3d). An inverse electron-demand also is observed when the complexing metal fragment is replaced by $Fe(CO)_3$ (reaction profiles for **11** with bis(trifluoromethyl)tetrazine, with cyclopentadiene, and with an electron-rich Danishefsky diene are included to Fig. S3 of the ESI†). The electron richness of the uncomplexed "ene" fragment in **14** also is evident from a significantly raised HOMO energy compared to benzene (note the relatively unchanged LUMO energy of **14** relative to benzene).

Conclusions

Metal-coordinated arenes containing "planar" aromatic fragments can exhibit aromaticity loss and reactivity gain depending on the nature of the complexed metal fragment. It is obvious, for the η^4-arenes, that metal complexation will distort the arene from planarity, and activate the leftover ene fragment. But the effect of aromaticity loss on reactivity is less intuitive for the η^2- and η^6-arenes, which remain largely planar upon metal coordination. We show here that aromaticity loss, but not distortion from planarity, is necessary for activating "ene-like" and "diene-like" reactivity in metal-complexed arenes. Our computational investigation demonstrates a protocol for how experimentalists might approach predicting ene-like and diene-like reactivity for transition metal coordinated arenes. NICS values can be convenient probes for predicting "ene-like" and "diene-like" reactivity in metal complexed arenes.

Computational methods

Geometry optimizations and frequency calculations were performed at ωB97X-D/def2-TZVPP//ωB97X-D/def2-SVP, employing Gaussian 16, Revision C.01.[35] The def2-SVP and def2-TZVPP basis sets include effective core potentials (ECPs) for atoms with $Z > 36$. Vibrational frequency analysis and intrinsic reaction coordinate (IRC) calculations verified the nature of the minima and transition state structures. Wiberg Bond Indices (WBIs) were computed using Natural Bond Orbital (NBO) Version 7.0.[36] HOMO–LUMO gaps (ΔE_{H-L}) were obtained from TD-DFT calculations at CAM-B3LYP/def2-TZVPP//ωB97X-D/def2-SVP. LUMO energies were derived by the sum of the computed HOMO energy and the ΔE_{H-L} energies. Nucleus-independent chemical shifts, $NICS(1)_{zz}$, were computed at ωB97X-D/def2-TZVPP. Bq points were placed at 1 Å above the ring centers opposite to the metal complexed face. $NICS(1)_{zz}$ values for the η^4-complexes were estimated by defining an *xy* plane with C1, C2, C4, and C5 (see ring carbon numbering for **9**, in Fig. 2).

Single-point energies for stationary points in the energetic profiles shown in Fig. 3 were computed at DLPNO-CCSD(T)/def2-TZVPP//ωB97X-D/def2-SVP using ORCA 5.0.[37] DFT functionals (ωB97X-D, PW6B95, M06, M06-L, MN15, PBE0-D3 all with def2-TZVPP) known to accurately simulate organometallic systems based on literature precedent[38] were tested against each other and benchmarked against data at the DLPNO-CCSD(T)/def2-TZVPP level. We found that ωB97X-D outperformed the other functionals in estimating activation barriers and reactions energies, and provided a reasonable cost-to-insight level that tracks well with what is reported by others.[39] Specifically, ωB97X-D/def2-TZVPP//ωB97X-D/def2-SVP yielded a free energy activation barrier ($\Delta G^{\ddagger}$) that is within 3 kcal mol^{-1} and a free energy of reaction that is within 1 kcal mol^{-1} of the DLPNO-CCSD(T)/def2-TZVPP//ωB97X-D/def2-SVP results. Images of

three-dimensional (3D) structures were produced using the CYLView20 software.[40]

Data availability

The data supporting this article have been included as part of the ESI.† Details of computational methods, Cartesian coordinates, and computed reaction barriers for alternative Diels–Alder reaction pathways are included to the ESI.†

Author contributions

J. V. S. conceptualized the project. J. V. S. and C. L. performed data analysis. Writing, editing, and investigation was performed by all authors. J. I. W. supervised the project.

Conflicts of interest

There are no conflicts to declare.

Acknowledgements

J. I. W. thanks the National Institute of General Medical Sciences (NIGMS) of the National Institutes of Health (NIH) (R35GM133548) and the Alfred P. Sloan Research Foundation (FG-2020-12811) for financial support. We acknowledge the use of the Carya cluster and support from the Research Computing Data Core at the University of Houston. We also thank Professor Thomas A. Albright and Dr Lucas Karas for friendly discussions.

Notes and references

1 W. Jarre, D. Bieniek and F. Korte, Benzene as Dienophile in the Diels-Alder Reaction, *Angew. Chem., Int. Ed.*, 1975, **14**, 181–182.
2 G. Seitz, R. H. Hoferichter and R. Mohr, Benzene and Linearly Annelated Arenes as Dienophiles in Diels–Alder Reactions with Inverse Electron Demand, *Angew. Chem., Int. Ed.*, 1987, **26**, 332–334.
3 C. Baralotto, M. Chanon and M. Julliard, Total Synthesis of the Tricyclic Sesquiterpene (±)-Ceratopicanol. An Illustration of the Holosynthon Concept, *J. Org. Chem.*, 1996, **61**, 3576–3577.
4 T. Gaich and J. Mulzer, From Silphinenes to Penifulvins: A Biomimetic Approach to Penifulvins B and C, *Org. Lett.*, 2010, **12**, 272–275.
5 R. Remy and C. G. Bochet, Arene–Alkene Cycloaddition, *Chem. Rev.*, 2016, **116**, 9816–9849.
6 J. J. Serrano-Pérez, F. de Vleeschouwer, F. De Proft, D. Mendive-Tapia, M. J. Bearpark and M. A. Robb, How the Conical Intersection Seam Controls Chemical Selectivity in the Photocycloaddition of Ethylene and Benzene, *J. Org. Chem.*, 2013, **78**, 1874–1886.
7 A. A. Aly, S. Ehrhardt, H. Hopf, I. Dix and P. G. Jones, Cycloadditions to Alkenyl[2.2]Paracyclophanes, *Eur. J. Org Chem.*, 2006, 335–350.
8 A. F. Murad, J. Kleinschroth and H. Hopf, Cyclophanes as Diene Components in Diels-Alder Reactions, *Angew. Chem., Int. Ed.*, 1980, **19**, 389–390.
9 Y. Inagaki, M. Nakamoto and A. Sekiguchi, A Diels-Alder Super Diene Breaking Benzene into C_2H_2 and C_4H_4 Units, *Nat. Commun.*, 2014, **5**, 3018.
10 E. P. Kündig, *Transition Metal Arene π-Complexes in Organic Synthesis and Catalysis*, Springer, Berlin and Heidelberg, Germany, 2004.
11 B. K. Liebova and W. D. Harman, Group 6 Dihapto-Coordinate Dearomatization Agents for Organic Synthesis, *Chem. Rev.*, 2017, **117**, 13721–13755.
12 L. J. Williams, Y. Bhonoah, L. A. Wilkinson and J. W. Walton, As Nice as π: Aromatic Reactions Activated by π-Coordination to Transition Metals, *Chem. –Eur. J.*, 2021, **27**, 3650–3660.
13 M. Jakoobi, Y. Tian, R. Boulatov and A. G. Sergeev, Reversible Insertion of Ir into Arene Ring C-C Bonds with Improved Regioselectivity at a Higher Reaction Temperature, *J. Am. Chem. Soc.*, 2019, **141**, 6048–6053.
14 A. P. Y. Chan, M. Jakoobi, C. Wang, R. T. O'Neill, G. S. S. Aydin, N. Halcovitch, R. Boulatov and A. G. Sergeev, Selective Ortho-C–H Activation in Arenes without Functional Groups, *J. Am. Chem. Soc.*, 2022, **144**, 11564–11568.
15 S. Lee, S. J. Geib and N. J. Cooper, [2 + 2 + 2] Addition of Diphenylketene to the Reductively Activated Benzene in the Transition Metal Complex [Mn(.eta.4-C6H6)(CO)3]- To Give a Dihydroisochroman-3-One, *J. Am. Chem. Soc.*, 1995, **117**, 9572–9573.
16 M. D. Chordia, P. L. Smith, S. H. Meiere, M. Sabat and W. D. Harman, A Facile Diels–Alder Reaction with Benzene: Synthesis of the Bicyclo[2.2.2]Octene Skeleton Promoted by Rhenium, *J. Am. Chem. Soc.*, 2001, **123**, 10756–10757.
17 P. M. Graham, S. H. Meiere, M. Sabat and W. D Harman, Dearomatization of Benzene, Deamidization of N,N-Dimethylformamide, and a Versatile New Tungsten π Base, *Organometallics*, 2003, **22**, 4364–4366.
18 L. Strausberg, M. Li, D. P. Harrison, W. H. Myers, M. Sabat and W. D. Harman, Exploiting the O- Quinodimethane Nature of Naphthalene: Cycloaddition Reactions with η^2-Coordinated Tungsten-Naphthalene Complexes, *Organometallics*, 2013, **32**, 915–925.
19 Q. H. Luu, T. Fiedler and J. A. Gladysz, Gigging Benzene, *Angew. Chem., Int. Ed.*, 2017, **129**, 5756–5758.
20 J. M. Keane and W. D Harman, A New Generation of π-Basic Dearomatization Agents, *Organometallics*, 2005, **24**, 1786–1798.
21 M. Franck-Neumann and D. Martina, Cycloadditions de la Tropone Avec le Cyclopentadiene: Synthese d'un Intermediaire Potentiel Par Utilisation de Complexe Metallique, *Tetrahedron Lett.*, 1977, **31**, 2293–2296.
22 J. H. Rigby and C. O. Ogbu, Tricarbonyl(Tropone)Iron as a Useful Functionalized Enone Equivalent, *Tetrahedron Lett.*, 1990, **31**, 3385–3388.

23 J. Clayden, N. Greeves and S. Warren, *Organic Chemistry*, Oxford University Press, Oxford, 2nd edn, 2012.
24 Z. Chen, C. S. Wannere, C. Corminboeuf, R. Puchta and P. v. R. Schleyer, Nucleus-Independent Chemical Shifts (NICS) as an Aromaticity Criterion, *Chem. Rev.*, 2005, **105**, 3842–3888.
25 Q. Zhu, S. Chen, D. Chen, L. Lin, K. Xiao, L. Zhao, M. Solà and J. Zhu, The Application of Aromaticity and Antiaromaticity to Reaction Mechanisms, *Fundam. Res.*, 2023, **3**, 926–993.
26 T. M. Krygowski, K. Ejsmont, B. T. Stepień, M. K. Cyrański, J. Poater and M. Solà, Relation between the Substituent Effect and Aromaticity, *J. Org. Chem.*, 2004, **69**, 6634–6640.
27 K. B. Wiberg, Application of the Pople-Santry-Segal CNDO Method to the Cyclopropylcarbinyl and Cyclobutyl Cation and to Bicyclobutane, *Tetrahedron*, 1968, **24**, 1083–1096.
28 F. Ding, M. T. Valahovic, J. M. Keane, M. R. Anstey, M. Sabat, C. O. Trindle and W. D. Harman, Diastereo- and Enantioselective Dearomatization of Rhenium-Bound Naphthalenes, *J. Org. Chem.*, 2004, **69**, 2257–2267.
29 C. A. Merlic, M. M. Miller, B. N. Hietbrink and K. N. Houk, Reactivity of (η^6-Arene)Tricarbonylchromium Complexes toward Additions of Anions, Cations, and Radicals, *J. Am. Chem. Soc.*, 2001, **123**, 4904–4918.
30 A. Lebcir, A. Boukhari, M. Solà and Y. García-Rodeja, [4+2]-Cycloaddition Reactions to Corannulene Accelerated by η^6 Coordination of Ruthenium Complexes, *Eur. J. Org Chem.*, 2024, e202400697.
31 P. v. R. Schleyer, B. Kiran, D. V. Simin and T. S. Sorensen, Does $Cr(CO)_3$ Complexation Reduce the Aromaticity of Benzene?, *J. Am. Chem. Soc.*, 2000, **122**, 510–513.
32 M. F. Semmelhack, W. Wulff and J. L. Garcia, New Substitution Eeactions on Indole Promoted by $Cr(CO)_3$ Unit, *J. Organomet. Chem.*, 1982, **240**, C5–C10.
33 D. Möhring, M. Nieger, B. Lewall and K. H. Dötz, Tricarbonyl(naphthoquinone)chromium: Synthesis and Application in [4+2] Cycloaddition Reactions, *Eur. J. Org Chem.*, 2005, 2620–2628.
34 T. M. Krygowski, Crystallographic studies of inter- and intramolecular interactions reflected in aromatic character of .pi.-electron systems, *J. Chem. Inf. Comput. Sci.*, 1993, **33**, 70–78.
35 M. J. Frisch, G. W. Trucks, H. B. Schlegel, G. E. Scuseria, M. A. Robb, J. R. Cheeseman, G. Scalmani, V. Barone, G. A. Petersson, H. Nakatsuji, X. Li, M. Caricato, A. V. Marenich, J. Bloino, B. G. Janesko, R. Gomperts, B. Mennucci, H. P. Hratchian, J. V. Ortiz, A. F. Izmaylov, J. L. Sonnenberg, D. Williams-Young, F. Ding, F. Lipparini, F. Egidi, J. Goings, B. Peng, A. Petrone, T. Henderson, D. Ranasinghe, V. G. Zakrzewski, J. Gao, N. Rega, G. Zheng, W. Liang, M. Hada, M. Ehara, K. Toyota, R. Fukuda, J. Hasegawa, M. Ishida, T. Nakajima, Y. Honda, O. Kitao, H. Nakai, T. Vreven, K. Throssell, J. A. Montgomery, Jr., J. E. Peralta, F. Ogliaro, M. J. Bearpark, J. J. Heyd, E. N. Brothers, K. N. Kudin, V. N. Staroverov, T. A. Keith, R. Kobayashi, J. Normand, K. Raghavachari, A. P. Rendell, J. C. Burant, S. S. Iyengar, J. Tomasi, M. Cossi, J. M. Millam, M. Klene, C. Adamo, R. Cammi, J. W. Ochterski, R. L. Martin, K. Morokuma, O. Farkas, J. B. Foresman, and D. J. Fox, *Gaussian 16*, Revision C.01, Gaussian, Inc., Wallingford CT, 2016.
36 E. D. Glendening, J. K. Badenhoop, A. E. Reed, J. E. Carpenter, J. A. Bohman, C. M. Morales, P. Karafiloglou, C. R. Landis and F. Weinhold, *NBO 7.0*, Theoretical Chemistry Institute, University of Wisconsin, Madison, 2018, **https://nbo7.chem.wisc.edu/**.
37 F. Neese, Software Update: The ORCA program System, Version 5.0, *Wiley Interdiscip. Rev.: Comput. Mol. Sci.*, 2018, **8**, 4–9.
38 T. Sperger, I. A. Sanhueza, I. Kalvet and F. Schoenebeck, Computational Studies of Synthetically Relevant Homogeneous Organometallic Catalysis Involving Ni, Pd, Ir, and Rh: An Overview of Commonly Employed DFT Methods and Mechanistic Insights, *Chem. Rev.*, 2015, **115**, 9532–9586.
39 M. Bursch, J.-M. Mewes, A. Hansen and S. Grimme, Best-Practice DFT Protocols for Basic Molecular Computational Chemistry, *Angew. Chem., Int. Ed.*, 2022, **61**, e202205735.
40 C. Y. Legault, *CYLview, 1.0b*, Université de Sherbrooke, 2009, **http://www.cylview.org**.